Correlation between the activation enthalpy and Kohlrausch exponent for ionic conductivity in alkali aluminogermanate glasses

K. L. Ngai
Naval Research Laboratory, Washington, D.C. 20375-5000

J. N. Mundy
Materials Science Division, Argonne National Laboratory, Argonne, Illinois 60439-4843

H. Jain
Department of Materials Science and Engineering, Lehigh University, Bethlehem, Pennsylvania 18015-3195

O. Kanert and G. Balzer-Jollenbeck
Institute of Physics, University of Dortmund, P.O. Box 50 05 00, D-4600 Dortmund 50, West Germany
(Received 2 August 1988)

The temperature and frequency dependence of electrical conductivity (σ_{dc}) and the electrical modulus of sodium, rubidium, and Na-Rb mixed alkali germanate and aluminogermanate glasses have been determined for varying alkali concentrations, and [Al]/[Ge] and [Na]/[Rb] ratios. In a few glasses the spin-lattice relaxation times T_1 for ^{23}Na have also been determined above room temperature. The frequency dependence of modulus is well fitted by the Kohlrausch ("stretched exponential" decay) function with exponent $\beta \equiv 1-n$ $(0<n<1)$ where n, according to the "coupling model," is a measure of ion-ion correlations. The microscopic activation energy, determined either directly from the temperature dependence of T_1 or as the product of $1-n$ and the activation energy of σ_{dc}, shows the best anticorrelation with n, as expected from the model.

I. INTRODUCTION

A large amount of structural information on alkali germanate glasses has accumulated over the past 20 years (Ref. 1 and references therein). The addition of an alkali oxide to GeO_2 glass converts some of the germanium from fourfold (tetrahedral) to sixfold (octahedral) coordination without breaking the Ge—O—Ge bridging bonds. In the $xNa_2O:(1-x)GeO_2$ series nonbridging oxygens (NBO) are formed at $x>0.18$. Above $x\sim 0.33$, the concentration of octahedrally coordinated Ge approaches zero and the germanate glass structure becomes analogous to the corresponding silicate glass structure. The structure of alkali aluminogermanate glasses, $xNa_2O:yAl_2O_3:(1-x-y)GeO_2$, has not been studied as extensively. Nevertheless, it is suggested that for [Al]/[Na]<1 substitution of Al_2O_3 transforms GeO_6 units presumably into GeO_4 units and eliminates nonbridging oxygens.[1] The parameters x and y in alkali aluminogermanate glasses offer an opportunity to vary alkali concentration and the structure over a large range with and without NBO's, and without any phase separation. Thus a study of ionic conductivity as a function of x and y will help us understand the effect of glass structure on ionic conduction processes. Our objective is to seek for an explicit correlation between the parameters which describe the electrical relaxation on the one hand and relate to the structure on the other.

Recently, Mundy and Jin[1] published comprehensive measurements of ac conductivity and tracer diffusivity in sodium aluminogermanate glasses with $x=0.01$, 0.05, 0.10, 0.15, 0.19, and 0.29 while keeping the [Al]/[Na] ratio at 0, 0.33, or 1.0. In the present work we present additional results and analyze the conductivity relaxation behavior for the mixed alkali system $xNa_2O:yRb_2O:zAl_2O_3:(1-x-y-z)GeO_2$ where x and y vary from 0.01 to 0.29 and z varies from 0.0 to 0.15. This allows us to study conductivity relaxation while changing the magnitude of conductivity but maintaining the same total alkali concentration. In the absence of any phase separation tendencies the alkali concentration may be related to the average alkali-alkali distance. Here electrical relaxation will be represented in the electrical modulus ($M^*\equiv 1/\epsilon^*$ where ϵ^* is the complex dielectric constant) formulism which has been used for alkali silicate,[2] single and mixed alkali borate,[3,4] alkali phosphate,[5] and alkali aluminoborate glasses[6] as well as for fused nitrate salts[7–11] and sodium β-alumina.[12]

II. THEORETICAL BACKGROUND

The dependence of M^* ($\equiv M'+iM''$) on frequency (ω) is given by[13]

$$M^*(\omega)=\epsilon_\infty^{-1}\left[1-\int_0^\infty dt\,\exp(-i\omega t)(-d\phi/dt)\right], \quad (1)$$

where ϵ_∞ is the high-frequency dielectric constant and $\phi(t)$ is the relaxation function. For an ideal dielectric $\phi(t)$ is a simple exponential describing the decay of electric field in the material, but for glasses such as those mentioned above $\phi(t)$ takes the form first suggested by

Kohlrausch in 1847 viz.,

$$\phi(t)=\exp[-(t/\tau^*)^{1-n}] , \tag{2}$$

where $0<n<1$ and τ^* is the relaxation time.[2-12] Both τ^* and n are material dependent. n may decrease slightly with increasing temperature but τ^* is strongly temperature dependent,[3]

$$\tau^*=\tau^*_\infty \exp(E_a^*/kT) . \tag{3}$$

An average relaxation time $\langle\tau^*\rangle$ can be obtained from the definition,

$$\langle\tau^*\rangle=\int\phi(t)\,dt$$
$$=[\Gamma(1-n)^{-1}]\tau^*/(1-n) , \tag{4}$$

where Γ is the gamma function. $\langle\tau^*\rangle$ is related to dc conductivity by the Maxwell's relation

$$\sigma_{dc}=e_0\epsilon_\infty/\langle\tau^*\rangle , \tag{5}$$

where e_0 is the permittivity of free space. This relation holds good for a variety of glasses and ionic conductors including the glasses discussed in this work.

From Eq. (2) we note that n describes the electrical relaxation process in the materials, which we would like to correlate with the structure. However, structure together with alkali concentrations is difficult to describe in compact terms. For this reason we may use τ^* or an activation energy E_a^* as a parameter to represent the structure. Our results will show that a correlation exists between n and E_a^*. In fact, a better correlation is found between n and E_a where

$$E_a=(1-n)E_a^* . \tag{6}$$

To understand the physical basis of this correlation and the meaning of E_a we must first briefly describe the coupling model of ionic conduction which also explains the general usefulness of the Kohlrausch function given in Eq. (2).

A. Coupling model

There are several versions of the coupling model which describe relaxation including conductivity relaxation in complex systems.[14-16] We restrict ourselves to a physical description only with the purpose of making it palpable that the model predicts an anticorrelation of the primitive activation energy E_a with the coupling parameter n, or equivalently a correlation between E_a and the fractional exponent

$$\beta\equiv 1-n \tag{7}$$

that appears in the Kohlrausch decay function.

The coupling model approaches the problem of the relaxation process corresponding to the jump of a cation in the presence of long range ion-ion interactions as follows. Initially, we consider each ion vibrating in a single-particle potential well. The vibration (attempt) frequency is determined by the vibrational force constant of the mobile cation motion fixed by the cation interaction with anions and other cations. For example, for glasses in which nonbridging oxygens are present, the frequency is determined by the cation-oxygen and cation-cation interactions. Associated with the potential well is the energy barrier E_a to the motion of ion between equivalent sites. The attempt frequency ν_∞ and the energy barrier (activation energy) E_a are called primitive in the coupling model because these quantities will be modified when interactions between cations and correlations of their motions are considered. The jump rate W_0 of an ion between two sites is given by the thermally activated form of

$$W_0\equiv\tau_0^{-1}=\nu_\infty\exp(-E_a/kT) . \tag{8}$$

W_0 is also called the primitive jump rate for the same reasons.

From general considerations, which is applicable to the present problem of a jumping ion correlated with other ions, we find that the ion jump rate is W_0 at short times but eventually, it will be slowed down by correlations with other ions to have the time-dependent form $W(t)$ given by

$$W(t)=\begin{cases} W_0 \text{ for } \omega_c t<1 & \text{(9a)} \\ W_0(\omega_c t)^{-n} \text{ for } \omega_c t>1 , & \text{(9b)} \end{cases}$$

where $0<n<1$ and ω_c is a frequency such that ω_c^{-1} is the time of the onset of the primitive rate slowing down. From earlier works, the order of magnitude of ω_c lies near or within the bounds of $10^{11}<\omega_c<10^{12}$ sec^{-1} for several oxide glasses. Once Eq. (9) is accepted, three coupled predictions[14] follow as consequences of solutions to the rate equation for the decay function $\phi(t)$:

$$d\phi(t)/dt=W(t)\phi(t) . \tag{10}$$

They are

$$(1)\quad \phi(t)=\exp[-(t/\tau^*)^{1-n}] \text{ for } \omega_c t>1 , \tag{11}$$

$$(2)\quad \phi(t)=\exp[-(t/\tau_0)] \text{ for } \omega_c t<1 , \tag{12}$$

$$(3)\quad \tau^*=[(1-n)\omega_c^n\tau_0]^{1/(1-n)} . \tag{13}$$

Combining Eqs. (8) and (13) gives

$$E_a=(1-n)E_a^* . \tag{14}$$

Detailed discussion and experimental tests of these coupled predictions can be found in recent reviews.[14-16]

Normally, one is accustomed to one activation energy E_a^*, that of dc conductivity, and it is believed to represent the well depth in the energetics of cation conduction process. However, according to the coupling model E_a is the actual or primitive energy barrier for ion jump and E_a^* arises in dc conduction due to ion-ion correlated motion. There are at least three methods of measuring E_a from experiments. The first is to measure σ_{dc} at very high temperatures where $\omega_c\tau_0\ll 1$ and, Eqs. (5) and (8) give

$$\sigma_{dc}=e_0\epsilon_\infty/\tau_0=e_0\epsilon_\infty\nu_\infty\exp(-E_a/kT) . \tag{15}$$

That is, the conductivity measurements at very high temperature will give E_a from the slope of Arrhenius plot.[4,17] The second method exploits the crossover from E_a^* to E_a via Brillouin scattering of ionic motion in the high-frequency range ($\sim$10 GHz). The crossover to

$\exp(-t/\tau_0)$ of the ion jump correlation function and an Arrhenius behavior with activation energy E_a of τ_0, in agreement with the predictions of the method, have been observed in such measurements on molten $0.4Ca(NO_3)_2$-$0.6KNO_3$ (Refs. 8 and 11) and in $(AgI)_x(AgPO_3)_{1-x}$ (Ref. 18) systems.

Recently, E_a has been directly observed from the measurements of nuclear spin relaxation in a variety of glasses.[19,20] The alkali ion nuclear spin lattice relaxation time T_1 has been measured as a function of temperature from 3 to $\sim$700 K. Above room temperature T_1 shows strong temperature dependence but weak dependence on Larmor frequency ω_L,

$$T_1^{-1} \sim \omega_L^{-m} \exp(-E_a/kT) , \tag{16}$$

where $0.5 \lesssim m \lesssim 0.8$. The results on several alkali borate, silicate, and germanate glasses have consistently shown E_a from T_1 data [Eq. (16)] to be the same as obtained from ac modulus data and Eq. (6).[21] The interpretation of Eq. (16) is that the nuclear spins relax when an alkali ion incorporated into a two-level system (TLS) assists the transition between the two levels by jumping to a neighboring site.[21] The transition between TLS's is proportional to the probability of an ion completing the jump and, therefore, the transition rate is thermally activated with energy barrier E_a. The sublinear Larmor frequency dependence of T_1^{-1} is a characteristic of spin relaxation involving TLS's.[22–25] Having determined E_a from T_1 measurements or modulus spectroscopy next let us investigate what kind of correlation between E_a or E_a^* and n is expected.

B. Correlation between Kohlrausch exponent and activation energy

The quantity n, also called the coupling parameter, appears in Eq. (9) as the fractional exponent of the rate slowing down function $f(t) \equiv (\omega_c t)^{-n}$, and is a measure of how important the correlations between ions are for relaxation. In the very low alkali concentration limit (less than a few 100 ppm) the average separation between alkalis is of the order of tens of angstroms. Correlations between ions are obviously unimportant because of large separation, and their effect on the single-ion jump relaxation process is also negligible. Hence, n should be zero or nearly zero and $E_a^* \cong E_a$. The entire decay function would be a single exponential, $\exp(-t/\tau_0)$, for all times which is in agreement with our analysis of electrical modulus data in the dilute alkali limit.

As alkali concentration is increased, the increasing correlation of the ionic motions is reflected by an increase in n and, from Eqs. (1) and (11), it follows that the electric modulus spectrum should broaden as observed in experiments with alkali glasses for x up to 50%. Martin and Angell[5,26] have illustrated this very nicely in glasses with nonbridging oxygens. They showed that since an increase in x leads to an increase in the concentrations of nonbridging oxygens and cation sites, the jump distance between sites will also decrease. The depth of the potential well, which is the primitive activation energy E_a in the coupling model, will decrease correspondingly (see Fig. 5 of Ref. 26). We emphasize that in the coupling model, the well depth of the potential-energy curve is identified with the primitive energy E_a and not with the activation energy E_a^* of dc conductivity (called E_{act} in Ref. 26).

It is important to point out that, on varying x, not only are the ions brought closer to each other to increase their correlations, but also there is an accompanying change in the energetics of the cation conduction process. The degree of correlation between ions is complicated by contributions from variations in both site proximity and well depth. The interplay between the ion-ion interaction and the single ion potential determines the correlation. One can expect a deeper well will increase the confinement of the ion's degree of freedom and diminish its correlation with others. The reduction of ion-ion correlation will cause a decrease in the constant n of the coupling model. In the levels structure approach,[27] for example, the reduction of ion-ion correlation will deplete the density of the "correlated states" and also decrease the coupling of a jumping ion with them. The quantity n being proportional to those two factors, hence, will decrease. In the Dirac's constraint dynamics approach reformulated in terms of a constrained complexity entropy, an entropy inequality has been used to show that the coupling parameter n decreases with reduction of ion-ion correlation.[28] Fortunately, as we shall see, the two concomitant variations, namely of site proximity and E_a, are reinforcing each other in the change of correlations between ions. Obviously, a simpler situation is to keep the site proximity constant and vary the well-depth E_a only by maintaining x near constant and changing the structure by altering the composition such as the $[Al_2O_3]/[B_2O_3]$ ratio in alkali aluminoborate glasses and $[Al_2O_3]/[GeO_2]$ ratio in alkali aluminogermanate glasses. In this way, we can modify the migration energy term of the total energy E_a caused by the necessary local volume expansion in the transition state connecting mobile cation sites. Another experiment, where only well depth changes, uses the mixed alkali effect wherein total alkali concentration is kept constant but E_a increases when the two alkalis are mixed.[19]

In the previous paragraph, we have considered the simplest situation of varying E_a while keeping site proximity (or alkali concentration) constant. In the more complicated situation an increase in x will increase the site proximity and decrease the well depth. Each of these changes tends to increase the ion-ion correlations and the value of n. Thus, the effects they have on the jump rate of an ion reinforce each other. An increase in n with concentration is expected. Angell[10] has noted an increase of n from zero to about one-half when x is increased from the dilute alkali limit to say 30% in silicate glasses.

III. RESULTS

A. Nuclear spin relaxation

The focus in this work is on the germanate and aluminogermanate glasses. For this reason, we present the ^{23}Na nuclear spin relaxation rate, $1/T_1$, measurements of

four $x\mathrm{Na_2O}:(1-x)\mathrm{GeO_2}$ glasses with $x=1.99$, 5.08, 8.83, and 15.61. The experimental procedure for T_1 measurements has been described in Ref. 29. Figure 1 is an Arrhenius plot of $1/T_1$ versus $1000/T$ in the high-temperature regime where the contribution to $1/T_1$ from transition of the two-level systems assisted by an ion jump, Eq. (16), dominates. The activation energy E_a is the microscopic energy barrier to an ion jump. The $1/T_1$ data at low temperatures representing spin relaxation caused by two-level excitations is not shown. The activation energies E_a determined from the slope of straight lines in Fig. 1 are listed in Table I together with the conductivity activation energy E_a^* from Ref. 1. It is clear by inspection that E_a and E_a^* differ greatly. The value of E_a has been also listed for each glass using Eq. (6) and n determined from electric modulus analysis of ac conductivity data. The two values of E_a agree very well and, thus, verify Eq. (6) as predicted by the coupling model. Considering the success of Eq. (6) we may now determine E_a simply from E_a^* and n obtained from ac measurements.[21]

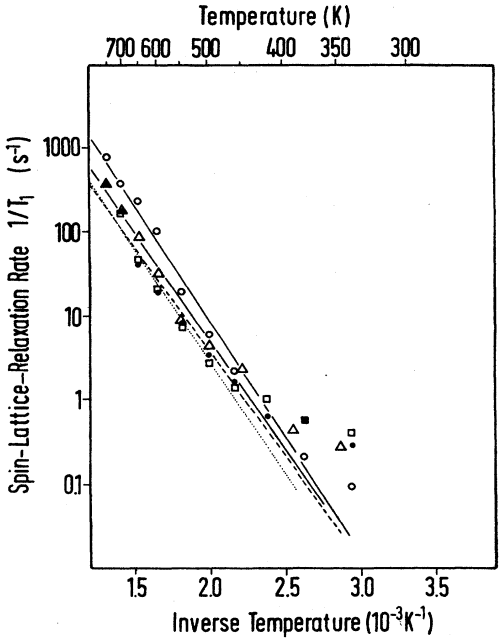

FIG. 1. ^{23}Na spin-lattice relaxation rate $1/T_1$ of a number of $x\mathrm{Na_2O}:(1-x)\mathrm{GeO_2}$ glasses plotted vs inverse of temperature (magnetic field $\beta_0=4.2T$). x in mol % for the samples is: (○), 1.99; (△), 5.08; (●), 8.83; and (□), 15.61; respectively.

B. Conductivity relaxation

The ac electrical conductivity of a large number of sodium, rubidium, and sodium-rubidium mixed alkali germanate and aluminogermanate glasses has been measured. Samples in Tables II–VII are labeled according to the following code:

(i) The first number is the sum of the nominal percentages of total alkali oxide and alumina.

(ii) Next, the letter designates the fraction of alumina in the first number, i.e., *A*: 0.0; *B*: 0.25, and *C*: 0.5.

(iii) The last number after multiplying with 10 designates the % fraction of rubidia in the total alkali oxide.

The dc conductivity was determined by the ac complex impedance method in order to avoid polarization effects resulting from the use of blocking electrodes. The glass sample and electrode preparations have been discussed in a previous work.[1] The complex impedance is measured over the frequency range of $20<f<10^5$ Hz. The main thrust of the previous papers has concerned the dc conductivity in the Na aluminogermanate glasses. Here we consider the wealth of ac conductivity data acquired in the course of the study as well as new dc and ac conductivity data on the rubidium and mixed alkali Na/Rb aluminogermanate glasses.

The ac conductivity data are analyzed in the electric modulus representation because of the advantages it offers,[13] and its direct connection to the conductivity relaxation function $\phi(t)$ through Eq. (1). For example, Fig. 2 shows typical imaginary part M'' of the complex modulus M^* for sample $5A10$ at $T=316.9\,^\circ\mathrm{C}$ and for $10C10$ at $T=373.8\,^\circ\mathrm{C}$. For each sample, data taken in a temperature range can be reduced to a master plot by shifting the M'' plots along the frequency axis, which is based on a direct connection of the ac phenomena to the dc conductivity. The shape of the M'' plot of data can be fitted rather well to a theoretical curve generated from

TABLE I. $x\mathrm{Na_2O}:(1-x)\mathrm{GeO_2}$. Comparison between the values of the primitive activation energy E_a deduced from the electric modulus data via the coupling model and measured directly by the spin-lattice relaxation. Not exactly the same samples are measured by ac conductivity and by spin-lattice relaxation. Comparisons are made between measurements on samples with compositions close to each other. The extreme left column are values of x for samples used in conductivity relaxation measurements. The extreme right column are values of x for samples used in nuclear spin-lattice relaxation measurements.

x mol %	E_a^* (eV)	n	$E_a=(1-n)E_a^*$ (eV) from coupling model	E_a (eV) from spin-lattice relaxation	x mol %
1.20	0.99	0.40	0.59	0.56	1.99
4.90	1.00	0.48	0.52	0.52	5.08
9.84	1.02	0.48	0.53	0.50	8.83
14.95	0.92	0.44	0.51	0.54	15.61

TABLE II. $x\mathrm{Rb_2O}:(1-x)\mathrm{GeO_2}$. Correlations of H, E_a^*, or E_a with n obtained by variation of the rubidium concentration.

Sample	x%	H (eV)	E_a^* (eV)	E_a (eV)	n
1*A*10	1.24[a]	1.481	1.4	1.19	0.15
5*A*10	4.9[b]	1.460	1.43	1.29	0.10
10*A*10	8.83	1.564	1.46	1.05	0.28
15*A*10	15.1	1.035	1.03	0.71	0.33–0.30[c]
22*A*10	21.9	0.835	0.80	0.48	0.44–0.35[c]
30*A*10	29.1	0.741	0.73	0.45	0.40–0.38[c]

[a]This sample contains 0.16% $\mathrm{Na_2O}$.
[b]This sample contains 0.19% $\mathrm{Na_2O}$.
[c]Temperature variation of n.

Eq. (12), with a choice of the fractional exponent $(1-n)\equiv\beta$. The solid curves in Fig. 2 with $n=0.1$ for 5*A*10 and $n=0.43$ for 10*C*10 are best fits to the data. Once n and τ^* (from the peak in M'' plot) are determined from this fitting procedure, the dc conductivity predicted by the electric modulus formalism is given in terms of τ^* and n by

$$\sigma_{dc}=e_0/M_\infty\langle\tau^*\rangle \tag{17}$$

and

$$\langle\tau^*\rangle=(\tau^*/\beta)\Gamma(1/\beta)\ , \tag{18}$$

where Γ denotes the gamma function. The agreement between such a value obtained for σ_{dc} and that obtained from complex impedance method is good at each temperature for all samples. Slight but systematic deviations of the M'' data from the theoretical curve are found at the high-frequency side of the peak. Figure 3 shows the deviation in the data of sample 20*A* at 137.7 °C and sample 40*C* at 66.9 °C as examples of the worst cases. Such deviation is common and found in the studies of many other systems.[5–12] An explanation has been suggested.[30]

The temperature dependence of τ^* is found to be well fitted to the Arrhenius equation

$$\tau^*=\tau_\infty^*\exp(E_a^*/kT)\ . \tag{19}$$

Generally, the σ_{dc} data are fitted to the equation

$$\sigma_{\mathrm{dc}}=(\sigma_0/T)\exp(-H/kT) \tag{20}$$

which includes a T^{-1} term in the pre-exponential. It must be pointed out that a careful analysis of extensive and precise dc conductivity data for well characterized alkali silicate glasses have indicated a better fit is obtained when no T^{-1} term is used.[31,32] The difference in the preexponential form for τ^* and σ_{dc} causes a difference between E_a^* determined from τ^* of modulus analysis and H from σ_{dc}, although the difference is often slight. For each glass, the pertinent quantities E_a^*, τ_∞^*, σ_0, H, n, etc., are obtained by the analyses of data in a range of temperature as described. The results are organized and presented in tables to be described next.

1. $x\mathrm{Rb_2O}:(1-x)\mathrm{GeO_2}$

The alkali concentration x is varied from about 1% to 30%. The results are summarized in Table II. The fractional exponent β and hence n is slightly temperature dependent for $x>15\%$. There is a slight decrease of n with increase in temperature as observed also in silicate and borate glasses. Whenever there is a significant variation of n with temperature, the range of variation is given in the table, and the average value is used for computation of E_a from Eq. (6). By inspection of Table II, we can see that as concentration is increased, on a gross scale, H, E_a^*, and E_a decrease while n increases. On a fine scale, one can see the variation of any of these quantities with x is not strictly monotonic. However, a plot of E_a versus n (Fig. 4) reveals a rather good anticorrelation between E_a and n expected from the coupling model (Sec. II),

TABLE III. $x\mathrm{Na_2O}:(1-x)\mathrm{GeO_2}$. Correlations of H, E_a^*, or E_a with n obtained by variation of the sodium concentration.

Sample	x%	H (eV)	E_a^* (eV)	E_a	n
TP	0.06	1.09	~1.09[a]	~1.09	0.00
1*A*	1.2	1.03	0.99	0.59	0.40
5*A*	4.9	1.08	1.00	0.52	0.48[c]
10*A*	9.84	1.08	1.02	0.53	0.48[c]
15*A*	14.95	0.97	0.92	0.51	0.44
20*A*	18.7[b]	0.87	0.83	0.46	0.44
30*A*	28.94	0.70	0.65	0.34	0.45

[a]Not sufficient data to establish E_a^*, value taken from H of Thomas and Peterson.
[b]This sample has 0.30% $\mathrm{Al_2O_3}$.
[c]Possibly an overestimate due to presence of a shoulder in the M'' versus $\log_{10}f$ plot.

TABLE IV. $x\mathrm{Na_2O}{:}y\mathrm{Al_2O_3}{:}(1-x-y)\mathrm{GeO_2}$. Correlations of H, E_a^*, or E_a with n obtained by maintaining x, the sodium concentration, constant and varying the concentration of Al_2O_3.

Sample	x%	y%	H (eV)	E_a^* (eV)	E_a (eV)	n
5*A*	4.90	0.00	1.08	1.00	0.51	0.50
10*C*	5.51	4.88	0.89	0.85	0.39	0.54
15*A*	14.95	0.00	0.97	0.92	0.51	0.44
20*D*	15.86	3.24	0.927	0.90	0.47	0.47
20*B*	14.65	5.11	0.946	0.87	0.44	0.50
30*C*	15.74	14.10	0.773	0.74	0.36	0.52
20*A*	18.68	0.30	0.87	0.83	0.46	0.43
30*B*	21.41	7.17	0.825	0.77	0.42	0.45
40*C*	20.53	18.77	0.695	0.65	0.30	0.53

whereas the anticorrelation between E_a^* or H with n is not as good (Fig. 4).

2. $xNa_2O{:}(1-x)GeO_2$

The very low alkali concentration sample with $x=0.06\%$ was measured by Thomas and Peterson.[33] From our analysis of their ac conductivity data, we find n is practically zero, in agreement with the low alkali silicate glasses studied by others.[10] There is a rapid rise of n to the value of 0.40 at $x=1.2\%$ and a subsequent gradual variation towards a constant value of about 0.45. The width of the M'' peak of samples 5*A* or 10*A* is larger than those of other samples, and this is reflected in a slightly larger value of n for these two. A close inspection of the M'' versus $\log_{10}f$ plots of these two samples has revealed the presence of a shoulder on the high-frequency side of the main peak. The origin of this shoulder, not present in other samples, is not clear at this time. These two samples may not be included into the consideration of the E_a or E_a^* versus n plot. Indeed if these two points are ignored, an anticorrelation between E_a and n is obtained (Fig. 5), similar to that seen in $x\mathrm{Rb}{:}(1-x)\mathrm{GeO_2}$.

3. $xNa_2O{:}yAl_2O_3{:}(1-x-y)GeO_2$ *x constant, y variable*

In Sec. II, we have discussed the best way to test the anticorrelation is to keep the alkali concentration and hence the alkali site proximity approximately constant and vary the Al_2O_3/GeO_2 ratio to change the well-depth. Results of a number of sodium aluminogermanate glasses are classified into several groups in which x is approximately constant, while y is varied. They are presented in Table IV. Anticorrelation with n is observed for E_a and E_a^* but not as well for H in all cases. Figure 6 shows the anticorrelation of E_a with n.

4. $xRb_2O{:}yAl_2O_3{:}(1-x-y)GeO_2$, *x constant, y variable*

The data are presented in the same format as for the sodium analogues. Results are summarized in Table V and the anticorrelation between E_a and n is depicted for the three separate pairs of samples in Fig. 7. Larger changes in both E_a and n are achieved with the addition of alumina in the rubidium glasses than in the sodium glasses.

5. $xNa_2O{:}yRb_2O{:}zAl_2O_3{:}(1-x-y-z)GeO_2$, *x and y constant, z variable*

Results of electric modulus analysis of ac conductivity data of mixed alkali aluminogermanate glasses are classified into six groups. In each group both x and y are held constant while z is varied. Again, the intent is to keep the site proximity approximately constant and change the well depth by varying the alumina to ger-

TABLE V. $x\mathrm{Rb_2O}{:}y\mathrm{Al_2O_3}{:}(1-x-y)\mathrm{GeO_2}$. Correlations of H, E_a^*, or E_a with n obtained by maintaining x, the rubidium concentration, constant and varying y, the concentration of Al_2O_3.

Sample	x%	y%	H (eV)	E_a^* (eV)	E_a (eV)	n
5*A*10	4.90[a]	0.00	1.46		1.30	0.10
10*C*10	4.68	4.68	1.19	1.15	0.66	0.43
10*A*10	8.83	0.00	1.56		1.12	0.28
20*C*10	9.27[b]	9.25		1.06	0.50	0.53
15*A*10	15.10	0.00	1.035		0.70	0.32
30*C*10	15.00	15.0	0.89	0.85	0.45	0.47

[a]This sample also contains 0.19 Na_2O.
[b]This sample also contains 0.24 Na_2O.

TABLE VI. $x Na_2O{:}y Rb_2O{:}z Al_2O_3{:}(1-x-y-z)GeO_2$. Correlations of E_a^* or E_a with n obtained by maintaining the alkali concentrations x and y separately constant and varying z, the concentration of Al_2O_3.

Sample	x%	y%	z%	E_a^* (eV)	E_a (eV)	n
15*A*3	10.5	4.5	0.0	1.14	0.63	0.45
20*B*3	10.5	4.5	5.0	1.17	0.59	0.50
30*C*3	10.5	4.5	15.0	0.87	0.41	0.53
15*A*5	7.5	7.5	0.0	1.23	0.71	0.42
20*B*5	7.5	7.5	5.0	1.17	0.63	0.46
30*C*5	7.5	7.5	15.0	0.96	0.51	0.47
15*A*7	4.5	10.5	0.0	1.29	0.72	0.44
20*B*7	4.5	10.5	5.0	1.30	0.70	0.46
30*C*7	4.5	10.5	15.0	0.99	0.51	0.48
10*A*3	7.0	3.0	0.0	1.15	0.62	0.46
20*C*3	7.0	3.0	10.0	0.84	0.39	0.54
10*A*5	5.0	5.0	0.0	1.36	0.90	0.34
20*C*5	5.0	5.0	10.0	0.97	0.55	0.43
10*A*7	3.0	7.0	0.0	1.30	0.72	0.45
20*C*7	3.0	7.0	10.0	1.09	0.58	0.47

mania ratio. The results are summarized in Table VI. The anticorrelation is evident for E_a and n (Fig. 8). It is not as satisfactory for E_a^* and n; the plot E_a^* versus n exhibits a weak maximum for two groups (Fig. 9).

6. $xNa_2O{:}yRb_2O{:}zAl_2O_3{:}(1-x-y-z)GeO_2$, x and y varying with $(x+y)$ and z constant

Here we keep $(x+y)$ and z both constant while varying x/y. This way of varying the "structure" is in the spirit of keeping both the site proximity and the structure sensitive Al_2O_3/GeO_2 ratio constant, and using the mixed alkali effect to change the effective well depth. No new information is sought here on the origin of the mixed alkali effect. We merely use it as a way to vary the ion transport property. Results of 23 glasses are classified into seven groups according to this method of analysis. The anticorrelation of E_a with n is observed in all cases except one. In going from 30*C*3 to 30*C*, E_a decreases from 0.41 to 0.37 eV while n also decreases from 0.53 to

TABLE VII. $x Na_2O{:}y Rb_2O{:}z Al_2O_3{:}(1-x-y-z)GeO_2$. Correlations of E_a^* or E_a with n obtained by varying x/y but keeping $x+y$ and z constant.

Sample	x%	y%	z%	E_a^* (eV)	E_a (eV)	n
10*B*7	2.25	5.25	2.5	1.38	0.83	0.40
10*B*3	5.25	2.25	2.5	1.03	0.52	0.50
10*C*10	0.0	4.68	4.68	1.15	0.66	0.43
10*C*5	2.5	2.5	5.0	0.98	0.53	0.46
10*C*3	3.5	1.5	5.0	0.92	0.46	0.50
10*C*	5.51	0.0	4.88	0.85	0.38	0.54
30*B*7	6.75	15.75	7.5	1.19	0.71	0.40
30*B*3	15.75	6.75	7.5	1.06	0.58	0.45
30*B*	24.41	0.0	7.17	0.77	0.42	0.45
30*C*7	4.5	10.5	15.0	0.99	0.53	0.47
30*C*10	0.0	15.0	15.0	0.85	0.45	0.47
30*C*3	10.5	4.5	15.0	0.87	0.41	0.53
30*C*	15.74	0.0	14.10	0.74	0.36	0.52
10*A*10	0.0	8.83	0.0	1.46	1.05	0.28
10*A*5	5.0	5.0	0.0	1.36	0.90	0.34
10*A*3	7.0	3.0	0.0	1.15	0.62	0.46
10*A*	9.84	0.0	0.0	1.02	0.51	0.50
20*B*7	4.5	10.5	5.0	1.32	0.71	0.46
20*B*3	10.5	4.5	5.0	1.17	0.59	0.50
20*B*	14.65	0.0	5.11	0.87	0.44	0.49
20*C*7	3.0	7.0	10.0	1.09	0.58	0.47
20*C*10	0.24	9.27	9.25	1.06	0.50	0.53
20*C*3	7.0	3.0	10.0	0.84	0.39	0.54

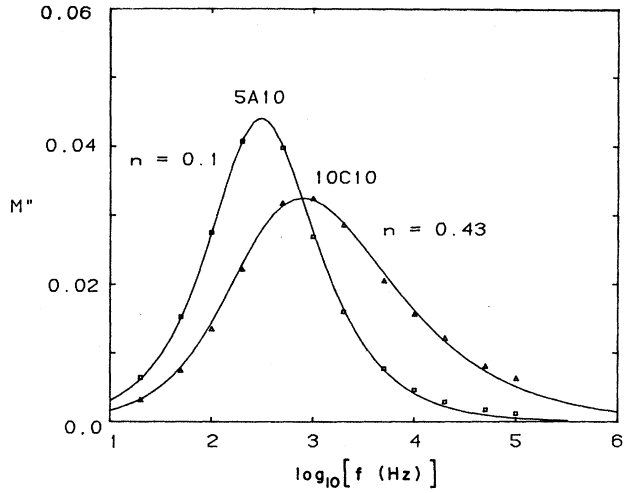

FIG. 2. Imaginary part of the electric modulus M'' of two Rb germanate glasses ($5A10$ and $10C10$) plotted vs logarithm to base 10 of frequency. The solid curves are the theoretical predictions by the Kohlrausch functions with the values of n as indicated. For compositions of the two glasses, see Table V.

0.51. Some representative anticorrelations are depicted in Fig. 10.

IV. DISCUSSION

As expected from the discussion in Sec. II B, the results on our sodium and rubidium germanate glasses (Tables II and III) confirm that n and, hence, correlation among ions increases with alkali content. This increase in n occurs both due to the changes in structure and the closer proximity of ions. The increase in n is stronger when the alkali ions are added first, but shows weaker

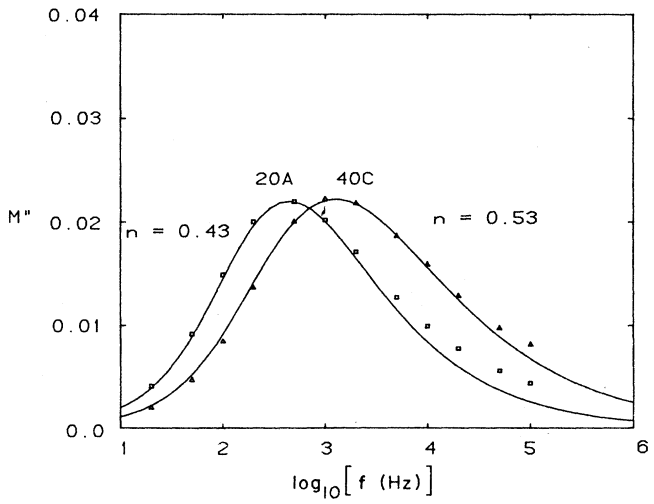

FIG. 3. Imaginary part of the electric modulus of two sodium germanate glasses ($20A$ and $40C$) plotted vs logarithm to base 10 of frequency. The solid curves are the theoretical predictions by the Kohlrausch functions with the values of n as indicated. For compositions of the two glasses, see Table IV.

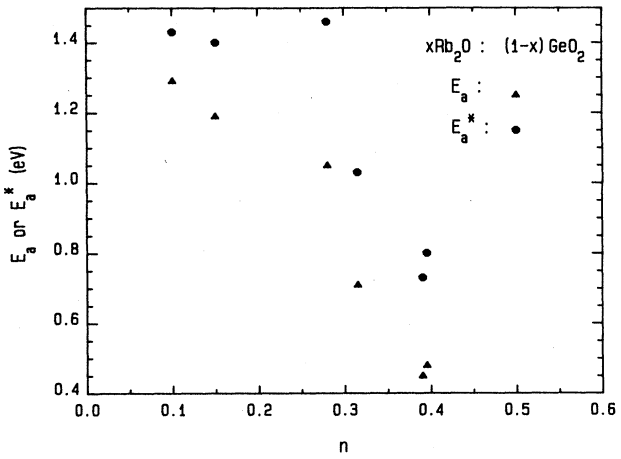

FIG. 4. Plot of the primitive activation energy E_a (▲) and E_a^* (●) vs n for different concentrations of Rb in Rb-germanate glasses. Note a stronger anticorrelation between E_a and n than between E_a^* and n.

dependence as the alkali content becomes high. In a simpler situation where the nominal alkali proximity is fixed but the structure is modified either by replacing Al for Ge or by using the mixed alkali effect (see various groupings in Tables IV–VII), n changes but by smaller amounts. However, within each grouping n anticorrelates with the activation enthalpies E_a, E_a^*, or H as shown in Figs. 4–10. Now the obvious question is: with which activation energy is the anticorrelation with n most meaningful? To address this question the experimental data and analysis can be viewed in two ways.

The first is entirely phenomenological in nature and restricts itself to basically a summary of the established facts. For all glasses, independent of alkali concentration and composition, the ac conductivity data when analyzed in the modulus representation is well fitted by the Kohlrausch function, Eq. (11), where the fractional exponent $\beta \equiv (1-n)$ and the effective relaxation time τ^* de-

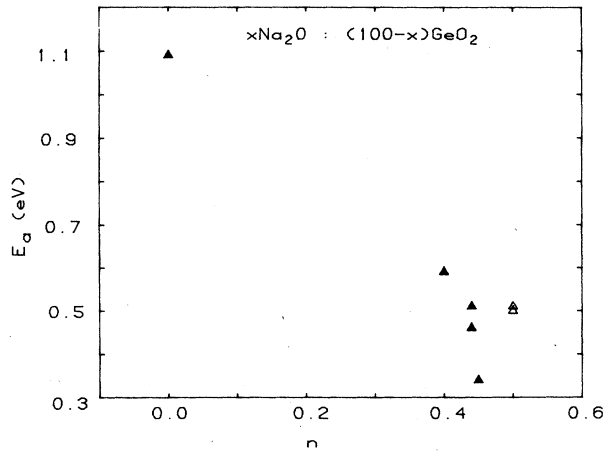

FIG. 5. Plot of the primitive activation energy E_a vs n for different concentrations of Na in Na-germanate glasses. Open triangles refer to samples $5A$ and $10A$. See footnote of Table III.

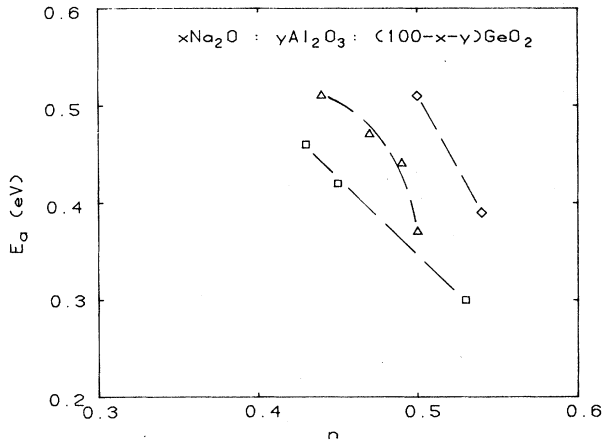

FIG. 6. Plot of the primitive activation energy E_a vs n for different proportions of alumina in Na-aluminogermanate glasses while the Na concentration is being kept constant to depict their strong anticorrelation. Data taken from Table IV. ◇ for $x \cong 5\%$; △ for $x \cong 15\%$; and □ for $x \cong 20\%$.

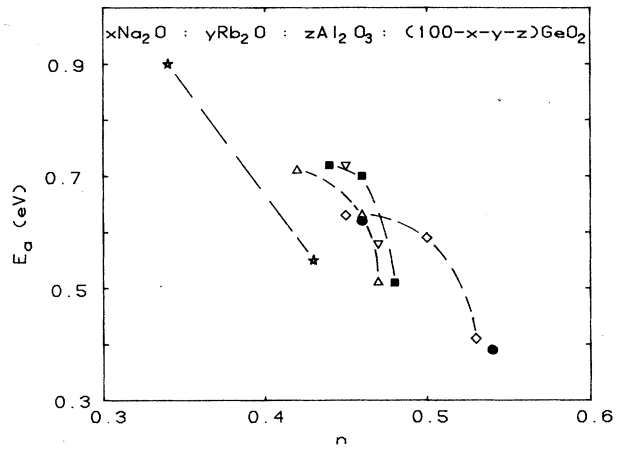

FIG. 8. Plot of E_a vs n for different proportions of alumina in mixed alkali (Na,Rb) aluminogermanate glasses $x\mathrm{Na_2O}$:$y\mathrm{Rb_2O}$:$z\mathrm{Al_2O_3}$:$(1-x-y-z)\mathrm{GeO_2}$ while the concentrations of Na and Rb are being kept constant to depict their strong anticorrelation. Data taken from Table VI. ◇ for $x=10.5\%$ and $y=4.5\%$; △ for $x=7.5\%$ and $y=7.5\%$; ■ for $x=4.5\%$ and $y=10.5\%$; ● for $x=7.0\%$ and $y=3.0\%$; ☆ for $x=5.0\%$ and $y=5.0\%$; and ▽ for $x=3.0\%$ and $y=7.0\%$.

pend on the glass. The dc conductivity σ_{dc} as well as τ^* have an Arrhenius temperature dependence. The activation energy H for σ_{dc} and E_a^* for τ^* are nearly the same, the slight difference is due to the conventional T^{-1} factor assumed in the preexponential of σ_{dc}. There is another activation energy E_a which is *directly observed* in the temperature dependence of the spin lattice relaxation rate $1/T_1$, Eq. (16). For all glasses in which both E_a^* and E_a have been measured and the Kohlrausch exponent β is known, the relation $E_a=\beta E_a^*$ is found to hold empirically. This is true also for silicate and borate glasses whenever both spin relaxation and conductivity measurements are available.[21] We have considered many different ways of selecting a pair of glasses in which the pair is related by a variation of either the alkali concentration or the glass structure via the $\mathrm{Al_2O_3/GeO_2}$ ratio, or by partial to complete replacement with a different alkali. Comparison is made for each pair of the quantities E_a^*, H, E_a, and β. A correlation between β and E_a^* or, β and H has been observed. An increase in β is accompanied by an increase in E_a^* and H. However, this correlation shows some minor exceptions. On the other hand, the correlation between β and E_a is strong and valid for almost all

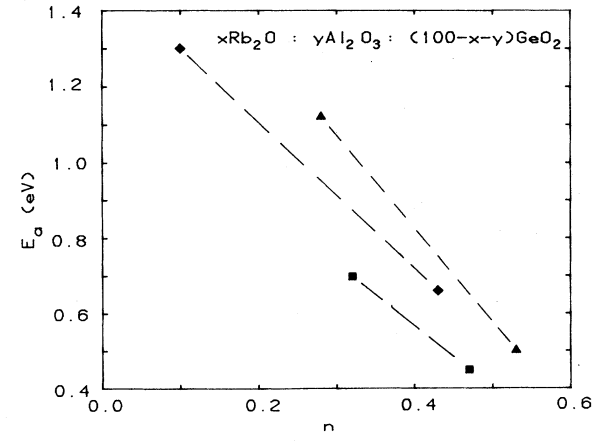

FIG. 7. Plot of the primitive activation energy E_a vs n for different proportions of alumina in Rb-aluminogermanate glasses while the concentration of Rb is being kept constant to depict their strong anticorrelation. Data taken from Table V. ◆ for $x \cong 5\%$; ▲ for $x \cong 9\%$; and ■ for $x \cong 15\%$.

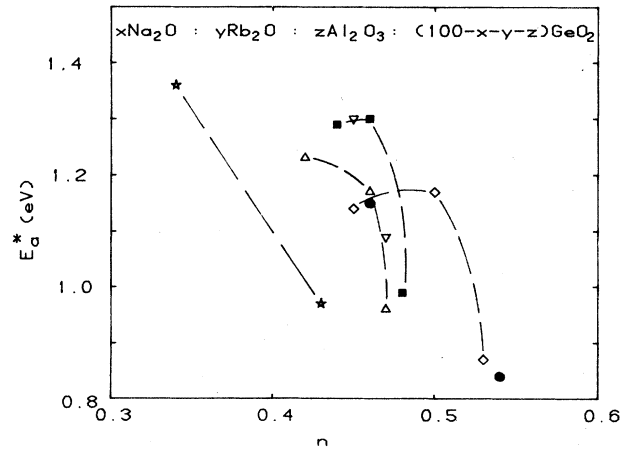

FIG. 9. Plot of the dc conductivity activation energy E_a^* vs n for different proportions of alumina in mixed alkali (Na,Rb) aluminogermanate glasses while the concentrations of Na and Rb are being kept constant to depict a weak anticorrelation between them. Data taken from Table VI. ◇ for $x=10.5\%$ and $y=4.5\%$; △ for $x=7.5\%$ and $y=7.5\%$; ■ for $x=4.5\%$ and $y=10.5\%$; ● for $x=7.0\%$ and $y=3.0\%$; ☆ for $x=5.0\%$ and $y=5.0\%$; and ▽ for $x=3.0\%$ and $y=7.0\%$.

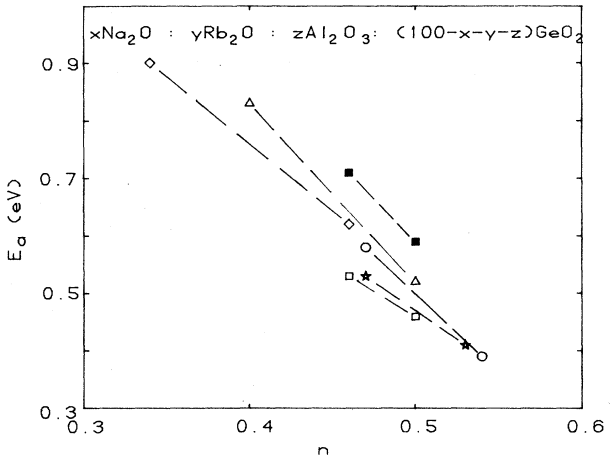

FIG. 10. Plot of E_a vs n for different mixed alkali aluminogermanate glasses by changing the Na to Rb ratio while maintaining the total alkali as well as the alumina concentration constant. Data taken from Table VII. △ for $z=2.5\%$ and $x+y=7.5\%$; ■ for $z=5.0\%$ and $x+y=15\%$; ◇ for $z=0.0\%$ and $x+y=10\%$; ○ for $z=10.0\%$ and $x+y=10\%$; ☆ for $z=15.0\%$ and $x+y=15\%$; and □ for $z=5.0\%$ and $x+y=5.0\%$.

pairs. Whenever a spin relaxation determination of E_a is not available, we identify E_a with the product βE_a^* where both β and E_a^* are obtained from the modulus analysis.

The second point of view originates theoretically from the coupling model and its predictions, augmented by a separate theory[21] of spin-lattice relaxation by two levels transition assisted by ion jump. The latter has identified the activation energy E_a observed by spin relaxation to be the well depth in the energetics of ion. Then the coupling model says the primitive ion jump rate $W_0=\nu_\infty \exp(-E_a/kT)$ is slowed down by correlations with other ions to have the time-dependent form $W_0(\omega_c t)^{-n}$ for $\omega_c t>1$. The exponent n correlates with the degree of correlations between ions which is lessened by an increase in single ion well depth E_a. Hence, the coupling model predicts n to inversely correlate with E_a.[28] From the relaxation rate $W(t)=W_0(\omega_c t)^{-n}$, it follows, as a consequence, the Kohlrausch relaxation function ϕ [Eq. (11)] and the effective relaxation time τ^* are related to τ_0 ($\equiv W_0^{-1}$) and ω_c by Eq. (13). A special consequence of this relation is that the ratio $E_a/(1-n)$ will be the activation energy E_a^* of τ^*. Since E_a^* is a "convolution" of E_a and n, we may not get a strong correlation between E_a^* and β although we have one between E_a and β. In this manner, we can give a satisfactory understanding not only of the essence of dc and ac conductivity, but also the strong anticorrelation between E_a and n observed in the large family of alkali germanate and aluminogermanate glasses. It is worthwhile to add that the same relations when applied to the isotope mass dependence of dc conductivity have successfully explained[13] the data of ^{7}Li and ^{6}Li borate glasses.[34] We are not aware of any other model of conductivity relaxation that can explain all these dynamic and steady state properties of ion transport. The strong correlation between E_a and β and the weak correlation between E_a^* and β established in this work will be an additional challenge for any model to explain.

V. CONCLUSIONS

The nonideal frequency dependence of electrical modulus of various alkali germanate and alkali aluminogermanate glasses has been fitted to the Kohlrausch function with exponent $\beta\equiv 1-n$ which depends on the glass. In terms of "coupling model" n describes correlations among various ions, and varies from 0 to 1 as the correlations increase. Our analysis shows that these correlations increase when the ion-ion proximity decreases and/or the primitive energy barrier for single ion uncorrelated hopping, E_a, decreases. E_a can be obtained directly from the temperature dependence of nuclear spin relaxation rates or calculated as the product of $1-n$ and the activation energy for electrical conductivity.

ACKNOWLEDGMENTS

This work is supported in part by U.S. Office of Naval Research (ONR) under Contract No. N0001488WX24074 (K.L.N.), by the U.S. Department of Energy (Division of Materials of the Office of Basic Energy Sciences) under Contract No. W-31-109-Eng-38 (J.N.M.), by the Deutsche Forschungsgemeinschaft (O.K. and G.B.J.), and an Alcoa Foundation grant (H.J.). We thank Dr. S. K. Chan and Dr. D. J. Lam of Argonne National Laboratory for bringing us together for this collaboration.

[1]J. N. Mundy and G. L. Jin, Solid State Ionics **21**, 305 (1986).
[2]L. P. Boesch and C. T. Moynihan, J. Non-Cryst. Solids **17**, 44 (1975).
[3]K. L. Ngai, R. W. Rendell, and H. Jain, Phys. Rev. B **30**, 2133 (1984).
[4]K. L. Ngai and H. Jain, Solid State Ionics **18&19**, 362 (1986).
[5]S. W. Martin and C. A. Angell, J. Non-Cryst. Solids **83**, 185 (1986).
[6]S. W. Martin, Ph.D. thesis, Purdue University, 1986 (unpublished).
[7]F. S. Howell, R. A. Bose, P. B. Macedo, and C. T. Moynihan, J. Phys. Chem. **78**, 639 (1974).
[8]C. A. Angell and L. M. Torell, J. Chem. Phys. **78**, 937 (1983).
[9]K. L. Ngai, Solid State Ionics **5**, 27 (1981).
[10]C. A. Angell, in *Relaxations in Complex Systems*, edited by K. L. Ngai and G. B. Wright (U.S. GPO, Washington, D.C.,

1985). Available from: National Technical Information Service, U.S. Department of Commerce, 5285 Port Royal Rd., Springfield, VA 22161.
[11]K. L. Ngai, A. K. Rajagopal, and C. Y. Huang, J. Appl. Phys. **55**, 1714 (1984).
[12]K. L. Ngai and U. Strom, Phys. Rev. B **27** 6031 (1983); Solid State Ionics **9&10**, 283 (1983).
[13]P. B. Macedo, C. T. Moynihan, and R. Bose, Phys. Chem. Glasses **13**, 171 (1972); V. Provenzano, L. P. Boesch, V. Volterra, C. T. Moynihan, and P. B. Macedo, J. Am. Ceram. Soc. **55**, 492 (1972).
[14]K. L. Ngai, R. W. Rendell, A. K. Rajagopal, and S. Teitler, Ann. (N.Y.) Acad. Sci. **484**, 150 (1986), and references quoted therein; IEEE Trans. Electron. Insulation **EI-21**, 313 (1986).
[15]A. K. Rajagopal and K. L. Ngai, in Ref. 10.
[16]K. L. Ngai, A. K. Rajagopal, and S. Teitler, J. Chem. Phys. **88**, 5086 (1988).
[17]C. A. Angell, Solid State Ionics **9&10**, 3 (1983).
[18]L. M. Torell, Phys. Rev. B **31**, 4103 (1985).
[19]H. Jain, G. Balzer-Jollenbeck, and O. Kanert, J. Am. Ceram. Soc. **68**, C24 (1985).
[20]G. Balzer-Jollenbeck, O. Kanert, and H. Jain, Collected Papers, XIV International Congress on Glass, New Delhi, 1986, Vol. 2, p. 186 (special publication of Indian Ceramic Society, Central Glass and Ceramic Research Institute, Calcutta 700 032, India).
[21]G. Balzer-Jollenbeck, O. Kanert, H. Jain, and K. L. Ngai, Phys. Rev. B **39**, 6071 (1989).
[22]J. Szeftel and H. Alloul, J. Non-Cryst. Solids **29**, 253 (1978).
[23]T. L. Reinecke and K. L. Ngai, Phys. Rev. B **12**, 3476 (1975).
[24]R. C. Zeller and R. O. Pohl, Phys. Rev. B **4**, 2029 (1971).
[25]G. Balzer-Jollenbeck, O. Kanert, J. Steinert, and H. Jain, Solid State Commun. **65**, 303 (1988).
[26]S. W. Martin, Solid State Ionics **18&19**, 472 (1986).
[27]K. L. Ngai, Comments Solid State Phys. **9**, 127 (1979); A. K. Rajagopal, S. Teitler, and K. L. Ngai, J. Phys. C **17**, 6611 (1984).
[28]K. L. Ngai, A. K. Rajagopal, and S. Teitler, Nucl. Phys. B (Proc. Suppl.) **5A**, 103 (1988).
[29]H. Selbach, O. Kanert, and D. Wolf, Phys. Rev. B **19**, 4435 (1979).
[30]K. L. Ngai and R. W. Rendell, in *Handbook of Conducting Polymers,* edited by T. A. Skotheim (Dekker, New York, 1986), Vol. II, p. 967.
[31]C. T. Moynihan, P. L. Gavin, and R. Syed, J. Phys. (Paris), Colloq. **43**, C9-391 (1982).
[32]H. Jain, J. Non-Cryst. Solids **66**, 517 (1984).
[33]M. P. Thomas and N. L. Peterson, Solid State Ionics **14**, 297 (1984).
[34]H. Jain and N. L. Peterson, Philos. Mag. A **46**, 351 (1982).